

Food & Function

Linking the chemistry and physics of food with health and nutrition

Accepted Manuscript

This article can be cited before page numbers have been issued, to do this please use: A. Celebioglu and T. Uyar, *Food Funct.*, 2020, DOI: 10.1039/D0FO01776K.



This is an Accepted Manuscript, which has been through the Royal Society of Chemistry peer review process and has been accepted for publication.

Accepted Manuscripts are published online shortly after acceptance, before technical editing, formatting and proof reading. Using this free service, authors can make their results available to the community, in citable form, before we publish the edited article. We will replace this Accepted Manuscript with the edited and formatted Advance Article as soon as it is available.

You can find more information about Accepted Manuscripts in the [Information for Authors](#).

Please note that technical editing may introduce minor changes to the text and/or graphics, which may alter content. The journal's standard [Terms & Conditions](#) and the [Ethical guidelines](#) still apply. In no event shall the Royal Society of Chemistry be held responsible for any errors or omissions in this Accepted Manuscript or any consequences arising from the use of any information it contains.

ARTICLE

Design of Polymer-free Vitamin-A acetate/Cyclodextrin Nanofibrous Webs: Antioxidant and Fast-dissolving Property

Asli Celebioglu* and Tamer Uyar*

Received 00th January 20xx,
Accepted 00th January 20xx

DOI: 10.1039/x0xx00000x

The encapsulation of food/dietary supplements into electrospun cyclodextrin (CD) inclusion complex nanofibers paves the way for developing novel carrying and delivery substance along with orally fast-dissolving property. In this study, CD inclusion complex nanofibers of Vitamin-A acetate were fabricated from the polymer-free aqueous systems by using electrospinning technique. The hydroxypropylated (HP) CD derivatives of HP β CD and HP γ CD were used for both encapsulation of Vitamin-A acetate and the electrospinning of free-standing nanofibrous webs. The ultimate Vitamin-A acetate/CD nanofibrous webs (NW) were obtained with the loading capacity of 5 % (w/w). The amorphous distribution of Vitamin-A acetate in the nanofibrous webs by inclusion complexation and the unique properties of nanofibers (e.g. high surface area and porosity) have ensured the fast-disintegration and dissolution/fast-release of Vitamin-A acetate/CD-NW in the saliva simulation and aqueous medium. The enhanced solubility of Vitamin-A acetate in case of Vitamin-A acetate/CD-NW has also ensured an improved antioxidant property for Vitamin-A acetate compound. Moreover, Vitamin-A acetate has thermally degraded at higher temperature in Vitamin-A acetate/CD-NW suggesting the enhanced thermal stability of this active compound. Here, HP β CD formed inclusion complexes in a more favorable way when compared to HP γ CD. Therefore, there were some uncomplexed Vitamin-A acetate crystals detected in Vitamin-A acetate/HP γ CD-NW, while Vitamin-A acetate molecules loaded in Vitamin-A acetate/HP β CD-NW were completely in complexed and amorph state. Depending on this, better solubilizing effect, higher release amount and enhanced antioxidant property have been provided for Vitamin-A acetate compound in case of Vitamin-A acetate/HP β CD-NW.

1. Introduction

The encapsulation of bioactive compounds such as vitamins, essential oils and flavors in functional food/dietary supplements is becoming an emerging research area.¹ The bioactive compounds are mostly hydrophobic with limited water solubility and they are often volatile and sensitive to environmental conditions.^{1,2} Therefore, encapsulation of such bioactive compounds within hydrophilic biopolymer matrices enhances their water solubility and bioavailability and also increase their shelf-life by improving their stability against temperature, light and oxygen.¹ There are several methods for encapsulation of bioactive compounds such as emulsion, extrusion, co-precipitation, coacervation, spray-drying, freeze-drying, electrospinning and electrospinning.^{1,3,4} Each encapsulation approach results in different structures and morphologies and therefore the physicochemical and delivery of these bioactive compounds would be different from each other. Among these encapsulation approaches, recently, electrospinning has also shown to be a very feasible one for encapsulation of bioactive compounds for various applications

including food, pharmaceutical and cosmetic.^{4–9} The solution electrospinning technique can enable the easy encapsulation of bioactive compounds by using their solution or dispersion with biopolymers at ambient conditions.^{4–9} On the other hand, the melt electrospinning which requires high temperature to melt polymer is a limited method, because there are few biopolymers that can be processed with high temperature. Moreover, high temperature can be problematic during melt electrospinning upon degrading and evaporating bioactive compounds.¹⁰ The electrospinning generally produces fibers with the diameter of less than micron and they are generally classified as nanofibers. The electrospun nanofibers are fabricated in the form of nonwoven having large surface area and highly porous structure.¹¹ Such lightweight, flexible, and free-standing nanofibrous webs which are electrospun from hydrophilic biopolymers can easily dissolve with water contact. Therefore, electrospun nanofibrous webs encapsulating bioactive compounds can be very feasible for developing fast-dissolving delivery systems for both food and pharmaceutical industries. Very recently, we have shown that the fast-dissolving nanofibrous webs of cyclodextrin inclusion complexes can be effectively produced from various compounds such as; essential oils^{12–17}, flavors^{18,19}, dietary supplements^{20–23}, and drugs^{24–27} in the absence of polymeric matrix. Cyclodextrins (CDs) are cyclic oligosaccharides obtained from starch and the U.S. Food and Drug Administration classified CDs as GRAS (Generally Recognized as Safe). CDs are

Department of Fiber Science & Apparel Design, College of Human Ecology, Cornell University, Ithaca, NY, 14853, USA.

*Corresponding Authors Email: AC: ac2873@cornell.edu; TU: tu46@cornell.edu
Electronic Supplementary Information (ESI) available: [details of any supplementary information available should be included here]. See DOI: 10.1039/x0xx00000x

quite applicable in both food and pharmaceutical industries due to their inclusion complexation ability and non-toxic nature.^{28,29} The molecular encapsulation of active ingredients through CD inclusion complexation could enhance the solubility and bioavailability, mask the bitter taste, control the release, extend the shelf-life and prevent their loss.^{28–31}

Vitamins have diverse biochemical functions and therefore they are used extensively in many areas including foods/feeds, pharmaceuticals, cosmetics, and biomedical applications.^{32,33} As one of the type of retinoids, Vitamin-A can be found in foods as retinyl ester (retinyl palmitate and retinyl acetate) or retinol form and they are commonly employed as food/dietary supplements and nutraceutical products due to their wide range of biochemical activities.^{34,35} As it has been reported previously, the most prominent property of Vitamin-A is its antioxidant capacity and therefore, it may show potential for treatments of cancer³⁶, diabetes³⁷, dermatological disorders³⁸ and cardiovascular diseases³⁹. Vitamin-A acetate (retinyl acetate) is one of the widely known and used derivatives of Vitamin-A having antioxidant property, however, it is lipophilic compound with very limited water solubility and is very sensitive to oxidation and high temperature. Therefore, encapsulation of Vitamin-A acetate is of interest for effective delivery of such bioactive compound to improve its bioavailability, stability and enhance its nutritional value. As it was mentioned, CDs are well-known as a molecular encapsulation agent due to their inclusion complexation property where the water solubility, bioavailability and stability of various bioactive molecules are significantly improved.⁴⁰ The inclusion complexation of Vitamin-A derivatives with different type of CD have been reported.^{41–43} The encapsulation of Vitamin-A acid⁴⁴, Vitamin-A palmitate^{45,46}, and Vitamin-A acetate⁴⁷ within polymeric electrospun nanofibers was also reported in order to control its delivery and/or increase its thermal stability. In the present study, we have aimed to develop the fast-dissolving and antioxidant nanofibrous webs of Vitamin-A acetate/CD inclusion complexes by using two derivatives of CD (hydroxypropyl-beta-cyclodextrin (HPβCD) and hydroxypropyl-gamma-cyclodextrin (HPγCD)) (Fig. 1). The structure, dissolution/disintegration, release, and the antioxidant potential of samples were examined by various analyses.

2. Materials and Methods

2.1. Materials

Hydroxypropyl-beta-cyclodextrin (HPβCD) (Cavasol W7 HP, DS: ~ 0.9) and Hydroxypropyl-gamma-cyclodextrin (HPγCD) (Cavasol W8 HP Pharma, DS: ~ 0.6) were presented by Wacker Chemie AG (USA). Vitamin-A acetate (retinol acetate, Sigma Aldrich), methanol (≥99.8% (GC), Sigma Aldrich), 2,2-diphenyl-1-picrylhydrazyl (DPPH, ≥97%, TCI America), sodium chloride (NaCl, >99%, Sigma Aldrich), o-phosphoric acid (85% (HPLC), potassium phosphate monobasic (KH₂PO₄, ≥99.0%, Fisher Chemical), sodium phosphate dibasic heptahydrate (Na₂HPO₄, 98.0-102.0%, Fisher Chemical), Fisher Chemical) and deuterated

dimethylsulfoxide (*d*₆-DMSO, 99.8%, Cambridge Isotope) were purchased and used as received. Millipore Milli-Q ultrapure water system (Millipore, USA) was used to supply high-quality distilled water.

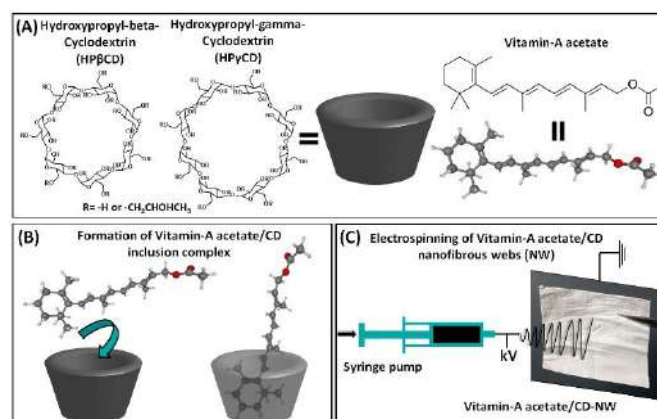


Fig. 1 (A) The chemical structure of HPβCD, HPγCD and Vitamin-A acetate. The schematic illustration of (B) Vitamin-A acetate and CD inclusion complex formation, and (C) the electrospinning of Vitamin-A acetate/CD-NW.

2.2. Electrospinning

For both pristine CD nanofibers and Vitamin-A acetate/CD-NW, the clear HPβCD and HPγCD solutions were initially prepared in distilled water by 200 % (w/v) CD concentration. In case of Vitamin-A acetate/CD-NW, Vitamin-A acetate powder was added to HPβCD and HPγCD solutions separately. The molar ratio of the Vitamin-A acetate/CD solutions were arranged as 1:2 (Vitamin-A acetate:CD) which correspond to the ~ 10 % (w/w, with respect to total sample amount) (~ 1 g CD and ~ 0.1 g Vitamin-A acetate) of Vitamin-A acetate content in Vitamin-A acetate/CD nanofibrous webs (NW). To ensure the inclusion complex formation, Vitamin-A acetate/CD aqueous systems were stirred for 24 hours (RT) by shielding from light sources. Prior the electrospinning, the conductivity (conductivity-meter; FiveEasy, Mettler Toledo, USA) and the viscosity (rheometer; AR 2000 rheometer, TA Instrument, USA (20 mm cone/plate spindle (CP 20-4, 4°); 0.01-1000 s⁻¹; 21 °C) of CD and Vitamin-A acetate/CD solutions were measured precisely. Electrospinning process was performed using electrospinning equipment (Spingenix, model: SG100, Palo Alto, USA). The solutions were filled into plastic syringes, separately fitted with 21 G metallic needle. Process parameters of flow rate, tip-to-collector distance, and high voltage were 0.5 mL/h, 12 cm and 15 kV, respectively (20 °C, 50 % relative humidity). The physical mixtures of Vitamin-A acetate/CD were prepared for the comparison, as well. Here, the pristine HPβCD-NW and HPγCD-NW (~25 mg) was homogenously blended with Vitamin-A acetate powder (~2.7 mg) to obtain Vitamin-A acetate/CD physical mixtures (PM) with the same molar ratio of 1:2 (Vitamin-A acetate:CD) used for the preparation of electrospinning system. The samples were stored at the ambient conditions (20 °C, 50 % relative humidity) during the analyses.

2.3. Morphology analyses

The morphology of electrospun HP β CD-NW, HP γ CD-NW, Vitamin-A acetate/HP β CD-NW and Vitamin-A acetate/HP γ CD-NW was analyzed using scanning electron microscope (SEM, Tescan MIRA3, Czech Republic) in high vacuum. The small piece of samples was fixed onto SEM stubs by double-sided carbon tape and sputter-coated with Au/Pd. For SEM imaging, the working distance was set to 10 mm and the accelerating voltage was 10 kV. The average diameter (AD) of nanofibers was calculated by the measurement of numerous fibers (~ 100) using ImageJ software.

2.4. Structural characterization

Attenuated total reflectance Fourier transform infrared (ATR-FTIR) spectrometer (PerkinElmer, USA) was used to get the Fourier transform infrared (FTIR) spectra of samples. The FTIR spectra were recorded at 4000-600 cm^{-1} region (resolution of 4 cm^{-1}) by 64 scans. X-ray diffractometer (Bruker D8 Advance ECO, USA) was used to investigate the X-ray diffraction pattern of the samples. The Cu-K α radiation source was used to form the XRD graphs (2 θ angles: 5 $^\circ$ and 30 $^\circ$) and voltage/current values were set to 40 kV/25 mA. The thermograms of samples were examined using differential scanning calorimeter (DSC, Q2000, TA Instruments, USA) (0 $^\circ\text{C}$ - 240 $^\circ\text{C}$; 10 $^\circ\text{C}/\text{min}$; N $_2$). The thermogravimetric analyzer (TGA, Q500, TA Instruments, USA) was utilized to determine the thermogravimetric profiles of samples (RT to 600 $^\circ\text{C}$; 20 $^\circ\text{C}/\text{min}$; N $_2$). Nuclear magnetic resonance spectrometer (Bruker AV500, with autosampler, USA) was utilized to calculate the molar ratio between Vitamin-A acetate and CD in Vitamin-A acetate/CD-NW. The *d*6-DMSO was used as the solvent to dissolve samples for proton nuclear magnetic resonance ($^1\text{H-NMR}$) measurements. The samples (~ 40 mg) were dissolved in *d*6-DMSO (~ 500 μL) and then they were loaded into instruments and $^1\text{H-NMR}$ spectra were recorded upon 16 scans. The chemical shifts (δ , ppm) of each sample were processed using Mestranova software.

2.5. Dissolution/disintegration, release, and phase solubility studies

For the examination of dissolution profile, ~ 10 mg of nanofibrous webs of pristine CD and Vitamin-A acetate/CD, and ~ 1 mg Vitamin-A acetate powder were located into glass vial, separately. Then, 5 mL of distilled water was poured into these vials in sequence (Video-S1). Here, the solubility enhancement of Vitamin-A acetate encapsulated in Vitamin-A acetate/CD-NW was also demonstrated spectroscopically (see supporting info). The time dependent release test of Vitamin-A acetate in Vitamin-A acetate/CD-NW (20 mg) was performed in distilled water (20 mL) at room temperature. For control, Vitamin-A acetate (~ 2 mg) powder was also examined using the initial Vitamin-A acetate content in nanofibrous webs. Here, Vitamin-A acetate/CD-NW and Vitamin-A acetate powder were placed into a beaker afterwards liquid medium was poured into samples. While the solution systems were being shaken (200 rpm), 500 μL of sample solution was withdrawn and then fresh medium (500 μL) was refilled at the determined time points. The released amount of Vitamin-A acetate was analyzed using UV-Vis-

spectroscopy (PerkinElmer, Lambda 35, USA). The calibration curve of Vitamin-A acetate showed linearity and acceptability with $R^2 > 0.99$. The measurement results were converted into released % by using this calibration curve. The experiments were performed three times and results were reported as mean \pm standard deviation. To evaluate the kinetic profile of samples, various mathematical models were applied including; zero and first-order release model, Higuchi release model and Korsmeyer-Peppas equation (see supporting information).⁴⁸

The disintegration profiles of Vitamin-A acetate/HP β CD-NW and Vitamin-A acetate/HP γ CD-NW were followed using the modified version of a technique which was previously conveyed by Bi et al.⁴⁹ In this approach, the physiological circumstances of the surface of a moist tongue is simulated. In this study, filter paper was firstly located in a plastic petri dish (10 cm), then wetted with artificial saliva (10 mL). 1.19 g Na $_2$ HPO $_4$, 0.095 g KH $_2$ PO $_4$ and 4 g NaCl were mixed in 500 mL distilled water and its pH was arranged to 6.8 with phosphoric acid to prepare artificial saliva. The extra artificial saliva was withdrawn from the petri dish and Vitamin-A acetate/CD-NW with approximate dimensions of ~ 3 cm X 5 cm was put at the centre of the filter paper (Video-S2).

The phase solubility profiles of Vitamin-A acetate/HP β CD and Vitamin-A acetate/HP γ CD systems were determined by the technique reported previously.⁵⁰ The excess amount of Vitamin-A acetate and CD (HP β CD and HP γ CD) powder with an increasing concentration from 0 to 40 mM were weighted into glass vials, separately. Afterwards, water (5 mL) was added each of the vial, they were sealed and shaken for 24 hours on incubator shaker (25 $^\circ\text{C}$ and 450 rpm) by shielding from the light. The PTFE filter (0.45 μm) was used to filter the incubated suspensions. UV-Vis-spectroscopy was used to measure the absorbance of the filtered aliquots. The experiments were conducted three times ($n=3$) and the phase solubility diagrams were plotted using the average absorption results. The binding constants (K_s) were determined from the below equation;

$$K_s = \text{slope}/S_0(1-\text{slope}) \quad (\text{Eq. 1})$$

where S_0 is the intrinsic solubility of Vitamin-A acetate (~ 7.25 μM) in the absence of CD.

2.6. Antioxidant activity test

The antioxidant activity of Vitamin-A acetate powder, Vitamin-A acetate/CD-NW and Vitamin-A acetate/CD-PM were examined using 2,2-diphenyl-1-picrylhydrazyl (DPPH) radical scavenging technique. For antioxidant experiment, Vitamin-A acetate/CD-NW (~ 30 mg), Vitamin-A acetate/CD-PM (~ 30 mg) and Vitamin-A acetate powder (~ 3 mg) were stirred in 2 mL of distilled water for 1 hour at 150 rpm. Then, all aqueous systems were filtered by PTFE filter (0.45 μm) to remove the undissolved Vitamin-A acetate parts in the solutions. Afterwards, 1 mL of the filtered solution of sample and 2 mL of 75 μM concentrated methanolic DPPH solution was mixed and incubated in the dark. The UV-Vis measurements were carried out at the different incubation time intervals and disappearance of DPPH absorption (517 nm) was followed to evaluate the inhibition performance of samples. Each experiment was

performed three times and the radical scavenging performance of samples were represented as inhibition percentage by using the below equation;

$$\text{Inhibition (\%)} = (A_{\text{control}} - A_{\text{sample}}) / A_{\text{control}} \times 100 \text{ (Eq. 2)}$$

where A_{control} stands for the absorbance values of control DPPH solution and A_{sample} stands for the sample solution one.

2.7. Statistical Analyses

The results of the replicated experiment ($n \geq 3$) were stated as mean values \pm standard deviations. The statistical analyses were performed using the one-way or two-way of variance (ANOVA). ANOVA analyses were carried out by OriginLab (Origin 2019, USA) (0.05 level of probability).

3. Results and discussion

3.1. Morphology analysis

Vitamin-A acetate molecules represent a lipophilic characteristic due to the cyclohexene ring and polyenic chain in the structure (Fig. 1).⁴¹ The lipophilic nature of Vitamin-A acetate is the major driving force for the inclusion complex formation with cyclodextrin (CD) molecules and as it was reported previously, the hydrophobic cyclohexene ring of Vitamin-A acetate is preferably encapsulated into the apolar cavity of CD in the event of inclusion complexation.⁴¹ In case of hydroxypropyl derivatives of CD, the extended cavity of CD enables the encapsulation of cyclohexene ring into the CD cavity, however the repulsion forces between the hydroxypropyl groups of CD and bended polyenic chain of Vitamin-A acetate can inhibit the effective association.⁴¹ Such that, for the interaction between Vitamin-A acetate and hydroxypropylated derivatives of CD, 1:2 molar ratio (Vitamin-A acetate:CD) has been recorded more favourable in which higher amount of CD molecules is used for the complex formation compared to 1:1 molar ratio (Vitamin-A acetate:CD).⁴¹ Therefore, we have preferred to prepare Vitamin-A acetate/CD aqueous solutions having 1:2 (Vitamin-A acetate:CD) molar ratio for the electrospinning. Here, the inclusion complex systems of Vitamin-A acetate/CD were obtained using two different modified CD types of hydroxypropyl-beta-cyclodextrin (HP β CD) and hydroxypropyl-gamma-cyclodextrins (HP γ CD). The highly concentrated solutions of CD (200%, w/v) ensure the electrospinning of uniform CD nanofibers, therefore Vitamin-A acetate/CD solutions were also prepared by using the 200 % (w/v) concentrated HP β CD and HP γ CD solutions. As it is seen in Fig. 2, the clear solutions of HP β CD and HP γ CD turned into yellowish colour by the addition of Vitamin-A acetate. Here, the high concentration and so the very high viscosity of Vitamin-A acetate/CD solutions (200 %, w/v) might hinder the efficient mixing of systems in order to attain an efficient inclusion complexation and so some uncomplexed Vitamin-A acetate might present in Vitamin-A acetate/CD nanofibrous webs (NW). Nevertheless, the electrospinning of Vitamin-A acetate/CD aqueous solutions prepared with 1:2 molar ratio was effective in which the uniform electrospun nanofibers of Vitamin-A

acetate/HP β CD and Vitamin-A acetate/HP γ CD were obtained upon self-standing and flexible properties (Fig. 2C, D-i). The uniform pristine HP β CD-NW and HP γ CD-NW were also produced in the form of self-standing character (Fig. 2A, B-i).

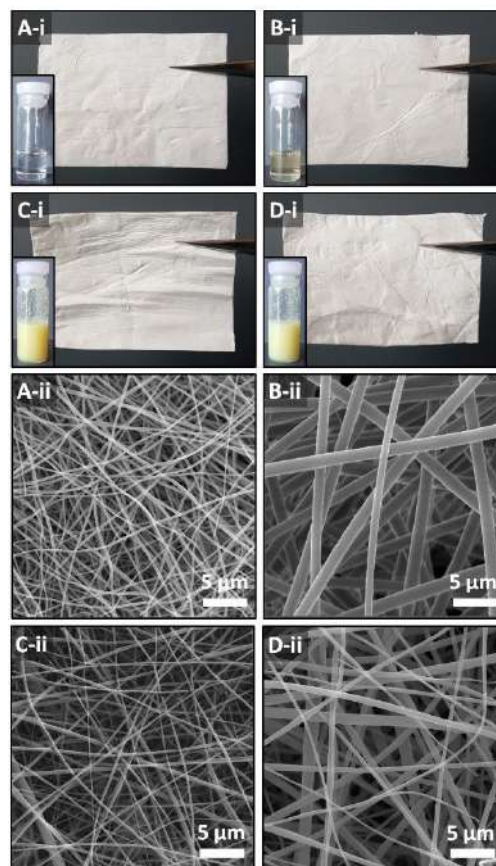


Fig. 2 (i) The photos of the electrospinning solutions and the free-standing webs and (ii) the representative SEM images of (A) HP β CD-NW, (B) HP γ CD-NW, (C) Vitamin-A acetate/HP β CD-NW (D) Vitamin-A acetate/HP γ CD-NW.

The SEM images depicted that the pristine CD-NW and the Vitamin-A acetate/CD-NW have uniform fibrous structure raised with bead-free morphology (Fig. 2). The solution properties (viscosity and conductivity) of the pristine CD and the Vitamin-A acetate/CD solutions, and the average diameter (AD) of the ultimate nanofibrous webs were given in Table S1. In electrospinning, solutions having higher viscosity and lower conductivity generally eventuate thicker fibers, because the electrospinning jet can be exposed less stretching compared to solutions having lower viscosity and higher conductivity during the electrospinning progression.⁵¹ The pristine HP β CD-NW and Vitamin-A acetate/HP β CD-NW were obtained having AD of 220 ± 60 nm and 195 ± 85 nm, respectively whereas the electrospinning of pristine HP γ CD-NW and Vitamin-A acetate/HP γ CD-NW resulted in much thicker fibers having AD of 1260 ± 245 nm and 610 ± 275 nm, respectively. HP β CD based solutions have higher conductivity along with lower viscosity compared to the HP γ CD based ones which probably provided higher stretching of electrospinning jet and so led to thinner fiber formation during the process (Table S1). When pristine CD

systems were compared with the Vitamin-A acetate/CD ones, it was observed that there was a decrease in the AD of CD-NW with the addition of Vitamin-A acetate. This might be due to the higher conductivity of Vitamin-A acetate/CD systems which can ensure higher stretching of jet during the process. In case of HP β CD systems, the conductivity of Vitamin-A acetate/HP β CD solution was slightly higher than pure HP β CD system, therefore there was not a distinct difference between the AD value of HP β CD-NW (220 \pm 60 nm) and Vitamin-A acetate/HP β CD-NW (195 \pm 85 nm). On the other hand, the variation between the AD of Vitamin-A acetate/HP γ CD-NW (1260 \pm 245 nm) and HP γ CD-NW (610 \pm 275 nm) was higher compared to HP β CD based systems due to the more significant difference between the conductivity values of Vitamin-A acetate/HP γ CD and HP γ CD solutions (Table S1). The statistical analyses supported our results in which variations were significantly detected between samples ($p < 0.05$).

3.2. Structural characterization

FTIR is commonly used technique to evaluate both the inclusion complex formation and the existence of guest molecules in inclusion complex structure.^{25,26} The interaction between guest molecules and CD cavities generally lead to disappearance, attenuation and/or shifts in the typical peaks of guest molecules.^{52,53} Fig. 3 indicated the FTIR spectra of Vitamin-A acetate powder, pristine CD-NW (HP β CD and HP γ -CD), Vitamin-A acetate/CD-NW (Vitamin-A acetate/HP β CD and Vitamin-A acetate/HP γ CD) and Vitamin-A acetate/CD physical mixtures (PM). There are major peaks at around 3000-3600 cm^{-1} for the primary/secondary -OH stretching, 2930 cm^{-1} for C-H stretching, 1650 cm^{-1} for O-H bending and 1370 cm^{-1} for -CH₃ bending vibrations of CDs (Fig 3A,B-i). The other major absorption bands which are seen between 1020 - 1200 cm^{-1} owing to coupled C-C/C-O and antisymmetric C-O-C stretching of CD.⁵⁴ In case of Vitamin-A acetate/CD-NW, the characteristic peaks of Vitamin-A acetate are not detectable since they were hindered due the encapsulation into CD cavities by inclusion complexation. On the other hand, the two characteristic peaks of Vitamin-A acetate locate at 1220 cm^{-1} and 1740 cm^{-1} corresponds to the stretching of C-C/C-C-H and C=O, respectively are obvious in the FTIR spectra of Vitamin-A acetate/CD-PM (Fig 3A,B-ii).^{55,56} This observation proved the inclusion complex formation between Vitamin-A acetate and CD molecules in Vitamin-A acetate/CD-NW.

As it is depicted in Fig. 4A-B, Vitamin-A acetate powder exhibits crystalline pattern and XRD provides useful information whether the Vitamin-A acetate molecules are distributed in the Vitamin-A acetate/CD nanofibrous webs as crystals or as amorphous state. In other words, XRD technique gives information about the complex formation between CD and guest molecules, because the guest molecules cannot aggregate to form crystalline and separate from each other when they are encapsulated in CD cavity by inclusion complexation.⁵² The XRD profiles of Vitamin-A acetate powder, Vitamin-A acetate/CD-NW and Vitamin-A acetate/CD-PM were displayed in Fig. 4A-B. The as-received Vitamin-A acetate

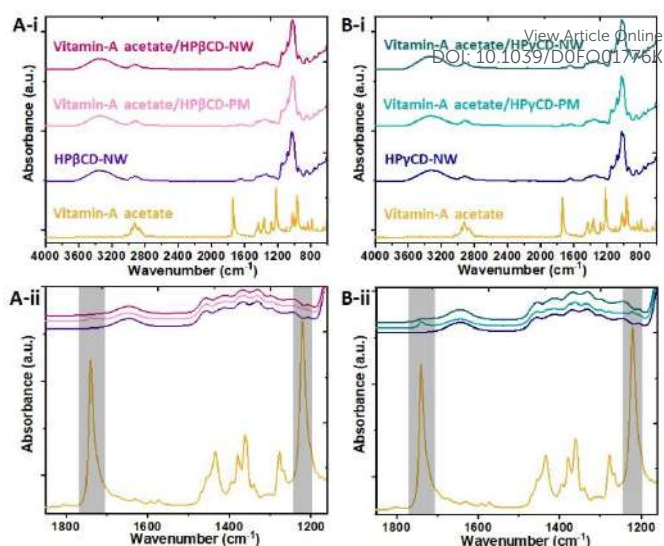


Fig. 3 (i) The full and (ii) the expanded range FTIR spectra of (A) Vitamin-A acetate powder, HP β CD-NW, Vitamin-A acetate/HP β CD-PM and Vitamin-A acetate/HP β CD-NW; (B) Vitamin-A acetate powder, HP γ CD-NW, Vitamin-A acetate/HP γ CD-PM and Vitamin-A acetate/HP γ CD-NW.

powder shows characteristic crystalline diffraction peaks at 9.1°, 17.3°, 18.5°, 20.1° and 24.4°. On the other hand, pristine HP β CD-NW and HP γ CD-NW have broad halo XRD pattern due to their amorphous nature (Fig. 4A-B). In case of Vitamin-A acetate/CD-PM, the crystalline peaks of Vitamin-A acetate become apparent because of uncomplexed structure of samples. Despite this, the Vitamin-A acetate/HP β CD-NW have amorphous pattern like pristine HP β CD-NW and Vitamin-A acetate/HP γ CD-NW indicates almost amorphous pattern with weak characteristic peaks (17.3°, 18.5° and 20.1°) of Vitamin-A acetate. The XRD pattern of Vitamin-A acetate/HP γ CD-NW showing the characteristic diffraction peaks of Vitamin-A acetate proves the existence of some crystal form of Vitamin-A acetate in this sample. On the other hand, Vitamin-A acetate was completely in the inclusion complex state in Vitamin-A acetate/HP β CD-NW. The Vitamin-A acetate crystals were not obvious in the SEM images of Vitamin-A acetate/HP γ CD-NW (Fig. 2D-ii) implying that the Vitamin-A acetate crystals were most probably distributed in small sizes within nanofibrous matrix.

The DSC data demonstrated that Vitamin-A acetate powder is in crystalline form having melting peak at 60 °C (Fig 4C-D). Therefore, DSC analysis was further performed to detect if there was any presence of uncomplexed crystalline Vitamin-A acetate in Vitamin-A acetate/CD-NW. The pristine HP β CD-NW and HP γ CD-NW have broad peak between 30-140 °C originated from water loss and since they are amorphous, there is no melting peak observed in the DSC thermogram of these samples.⁵⁷ For Vitamin-A acetate/HP β CD-NW, the melting peak of Vitamin-A acetate was not detected confirming the fully inclusion complexed state of Vitamin-A acetate with HP β CD in this sample. The guest molecules are separated from each other and not able to form crystals in case of inclusion complexation, therefore the characteristic melting peak of guest molecules is

not detected in DSC data.⁵² On the other hand, the DSC of Vitamin-A acetate/HP β CD-PM indicates endothermic peak at 59 °C with a peak area of 5.8 J/g (Fig. 4C). In case of Vitamin-A acetate/HP γ CD-NW, there is very small endothermic peak at 56 °C for melting of Vitamin-A acetate crystals with a peak area of ~ 0.9 J/g. The physical mixture of Vitamin-A acetate/HP γ CD has endothermic peak at 59 °C with a peak area of 5.1 J/g (Fig. 4D). This finding revealed that most of the Vitamin-A acetate was inclusion complexed with HP γ CD, but there were still uncomplexed Vitamin-A acetate crystals present in Vitamin-A acetate/HP γ CD-NW. The DSC results further proved that the Vitamin-A acetate was completely in inclusion complex state in Vitamin-A acetate/HP β CD-NW whereas there was uncomplexed crystalline Vitamin-A acetate present in Vitamin-A acetate/HP γ CD-NW. Briefly, DSC findings are in good agreement with the XRD data.

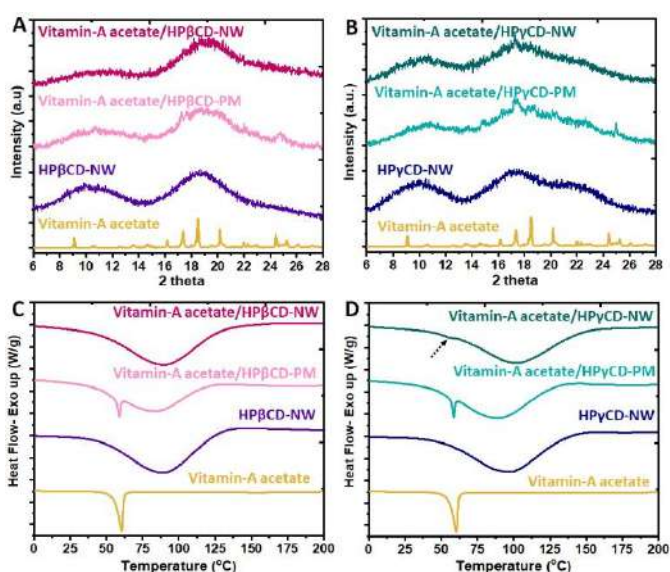


Fig. 4 (A, B) XRD graphs and (C, D) DSC thermograms of Vitamin-A acetate powder, HP β CD-NW, Vitamin-A acetate/HP β CD-PM, Vitamin-A acetate/HP β CD-NW and HP γ CD-NW, Vitamin-A acetate/HP γ CD-PM, Vitamin-A acetate/HP γ CD-NW.

The TGA measurements of Vitamin-A acetate powder, pristine CD-NW, Vitamin-A acetate/CD-NW and Vitamin-A acetate/CD-PM were performed by thermogravimetric analyzer (TGA) (Fig. 5). The Vitamin-A acetate powder displays mass loss that starts at 100 °C and ends up at 500 °C by two degradation steps. The pristine CD-NW have initial weight (%) loss below 100 °C due to the evaporation of water. The pristine HP β CD-NW and HP γ CD-NW exhibit main thermal degradation in the ranges of 280-430 °C and 265-420 °C, respectively. The main degradation of Vitamin-A acetate overlaps with the main degradation step of pristine CD (Fig. 5), therefore two steps of mass losses were also observed in case of Vitamin-A acetate/CD-NW samples. In addition, the first degradation step of Vitamin-A acetate powder, which occurs at lower temperature range (100 °C-276 °C) is not obvious for Vitamin-A acetate/CD-NW and this might be an evidence for the inclusion complex formation between Vitamin-A acetate and CD molecules (Fig. 5). The inclusion complexation can principally increase the thermal stability of

guest molecules and this is observed by shifting of the thermal degradation step of guest to the higher temperature ranges.⁵² On the other hand, the considered degradation step of Vitamin-A acetate is detected for Vitamin-A acetate/CD-PM. In brief, TGA findings validated the interaction between Vitamin-A acetate and CD in Vitamin-A acetate/CD-NW.

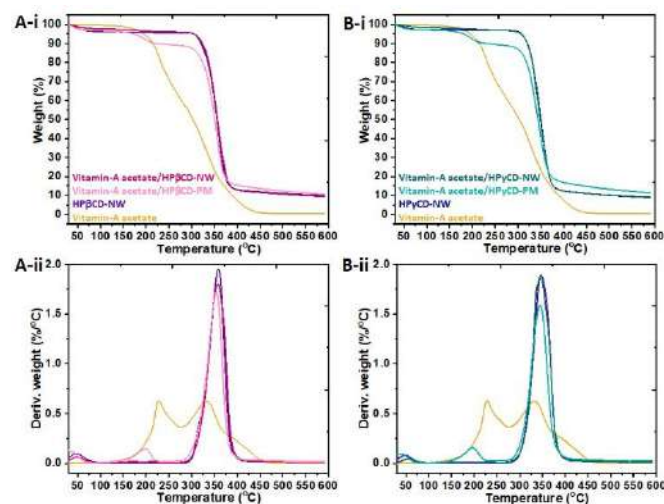


Fig. 5 TGA thermograms (i) and derivatives (ii) of (A) Vitamin-A acetate, HP β CD-NW, Vitamin-A acetate/HP β CD-NW, Vitamin-A acetate/HP β CD-PM and (B) Vitamin-A acetate, HP γ CD-NW, Vitamin-A acetate/HP γ CD-NW, Vitamin-A acetate/HP γ CD-PM.

In this study, ¹H-NMR measurements were performed in order to determine the molar ratio between Vitamin-A acetate and CD in Vitamin-A acetate/CD-NW which can be used to calculate the loading efficiency of Vitamin-A acetate/CD-NW (Fig. 6 and Fig. S1). The electrospinning solution systems of Vitamin-A acetate/CD were prepared by the initial molar ratio of 1:2 (Vitamin-A acetate:CD) for both Vitamin-A acetate/HP β CD and Vitamin-A acetate/HP γ CD. Here, Vitamin-A acetate powder, Vitamin-A acetate/HP β CD-NW and Vitamin-A acetate/HP γ CD-NW were dissolved in *d*₆-DMSO before the ¹H-NMR measurements. The taken spectra of the samples were depicted in Fig. 6 and Fig. S1. The molar ratio between Vitamin-A acetate and CD was calculated by using the integration proportion of the characteristic peaks of Vitamin-A acetate and CD in Vitamin-A acetate/CD-NW. The -CH₃ peaks of both Vitamin-A acetate peaks at 1.3-2.1 ppm and modified CDs at 1.03 ppm were used for the calculation of molar ratio. As it is seen, the -CH₃ peaks of Vitamin-A acetate located at ~ 1 ppm overlaps with the CD ones. Therefore, for this region, the integration value of Vitamin-A acetate was subtracted from the integration value of Vitamin-A acetate/CD-NW during the calculations. The molar ratios of Vitamin-A acetate/HP β CD-NW and Vitamin-A acetate/HP γ CD-NW were determined as ~ 1:4 from the ¹H-NMR peak integrations. The ¹H-NMR findings indicated that the ~ 50 % of the initial Vitamin-A acetate concentration were conserved during the electrospinning of Vitamin-A acetate/CD-NW and so, the ultimate nanofibrous webs were obtained by ~ 5 % (w/w) loading capacity. Here, the highly viscous Vitamin-A acetate/CD solution which have been

prepared using high CD concentration (200 %, w/w) might raise some difficulties during the stirring of system. Therefore, the initial content of Vitamin-A acetate (~ 10 %, w/w) could not be completely preserved during the preparation steps and some parts of Vitamin-A acetate could not be included into the electrospinning process. On the other hand, the loaded Vitamin-A acetate amount of ~ 5 % (w/w) into the nanofibrous webs is quite enough to obtain an efficient antioxidant performance as it will be discussed in the following part. As it was addressed in the previous section, there are some uncomplexed Vitamin-A acetate in Vitamin-A acetate/HP γ CD-NW, however *d*₆-DMSO enabled to dissolve both complexed and uncomplexed type of Vitamin-A acetate present in this nanofibrous webs. It is also worth to mention that, Vitamin-A acetate/HP β CD-NW and Vitamin-A acetate/HP γ CD-NW have the same Vitamin-A acetate peaks with pure Vitamin-A acetate powder that explained that the structure of Vitamin-A acetate was protected during the electrospinning process.

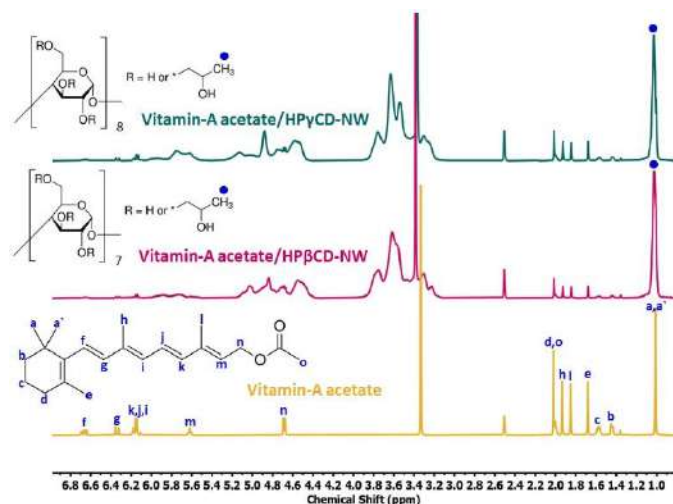


Fig. 6 $^1\text{H-NMR}$ spectra of Vitamin-A acetate powder, Vitamin-A acetate/HP β CD-NW and Vitamin-A acetate/HP γ CD-NW which were recorded by dissolving samples in *d*₆-DMSO.

3.3. Dissolution, release, and disintegration profile

The fast dissolution profile of Vitamin-A acetate powder (~ 1 mg), pristine CD-NW (~ 10 mg) and Vitamin-A acetate/CD-NW (~ 10 mg) were visually examined by adding 5 mL of water to the vials which were loaded with the mentioned samples (Fig. 7 and Video S1). Here, pristine HP β CD-NW and HP γ CD-NW disappeared upon the contact of water. On the other hand, Vitamin-A acetate did not dissolve and remained on the top of water over given period of time because of its almost insoluble nature (Fig. 7). In case of Vitamin-A acetate/HP β CD-NW, sample disappeared immediately by the addition of water, however a slightly turbid aqueous system was obtained, since the ultimate complex structure of the Vitamin-A acetate/HP β CD most probably indicated low solubility in water for the tested sample concentration (2 mg/mL). Even so, the Vitamin-A acetate/HP β CD inclusion complexes homogeneously dispersed in water (Fig. 7). On the contrary, the un-complexed and undissolved Vitamin-A acetate content in Vitamin-A

acetate/HP γ CD-NW were a bit heterogeneously detected in the water. Here, the solubility enhancement of Vitamin-A acetate in Vitamin-A acetate/CD-NW were also indicated using spectroscopic measurement. The same amount of Vitamin-A acetate powder (~ 1 mg) and Vitamin-A acetate/CD-NW (~ 10 mg) were stirred in 5 mL water for 1 hour and then the undissolved parts of Vitamin-A acetate were removed by filtration. Fig. S2 showed the UV-Vis absorbance graphs of the filtered solutions. It is obvious that, Vitamin-A acetate has a very low absorbance intensity in the given range because of its quite poor water solubility (~ 7.5 μM). On the other hand, the solution of Vitamin-A acetate/CD-NW indicated extremely higher intensity compared to Vitamin-A acetate powder (Fig. S2), despite the fact that, they contain less amount of Vitamin-A acetate (~ 0.5 mg) compared the Vitamin-A acetate powder (~ 1 mg) used for this experiment. This finding has proved the enhanced solubility of Vitamin-A acetate in Vitamin-A acetate/CD-NW by inclusion complexation. Even, Vitamin-A acetate/HP β CD-NW and Vitamin-A acetate/HP γ CD-NW were obtained with the same loading capacity (5 %, w/w) of Vitamin-A acetate, the absorbance intensity of Vitamin-A acetate/HP β CD solution is higher than Vitamin-A acetate/HP γ CD one (Fig. S2). The reason for this is the uncomplexed/undissolved Vitamin-A acetate parts present in Vitamin-A acetate/HP γ CD-NW and this suggest that HP β CD can provide a better solubility enhancement for Vitamin-A acetate than HP γ CD.



Fig. 7 The dissolution behaviour of samples in water. (A) Vitamin-A acetate powder, (B) HP β CD-NW, (C) Vitamin-A acetate/HP β CD-NW, (D) HP γ CD-NW and (E) Vitamin-A acetate/HP γ CD-NW. These pictures were captured from Video S1.

In this study, the time dependent release profile of Vitamin-A acetate powder, Vitamin-A acetate/HP β CD-NW and Vitamin-A acetate/HP γ CD-NW was examined, as well (Fig. 8). The significant improvement of release of Vitamin-A acetate in the nanofibrous webs was demonstrated compared to pure Vitamin-A acetate (Fig. 8). Both Vitamin-A acetate/CD-NW dissolved instantly with the contact of liquid medium and showed similar release profiles. Vitamin-A acetate/HP β CD-NW and Vitamin-A acetate/HP γ CD-NW respectively released 94.3 \pm 4.9 % and 55.2 \pm 1.3 % of the encapsulated Vitamin-A acetate in the first 30 seconds and indicated approximately steady profile up to the 10 minutes. This finding was correlated with the dissolution test in which Vitamin-A acetate/HP γ CD-NW showed lower absorbance intensity compared to Vitamin-A acetate/HP β CD-NW at the end of 1 hour stirring period (Fig. S2) due to the uncomplexed/undissolved Vitamin-A acetate part in Vitamin-A acetate/HP γ CD-NW. On the other hand, Vitamin-A acetate powder was almost not freed into the liquid medium in this given period (10 minutes, \sim 0.10 \pm 0.07 %). This results also confirmed that the inclusion complex formation between Vitamin-A acetate and CD within the Vitamin-A acetate/CD-NW ensured a distinct enhancement of the release profile of this active compound compared to its pristine form of powder. Here, the statistical analyses showed the significant variations between samples with $p < 0.05$ value. The release behaviours of samples were also evaluated using different kinetic models. The correlation coefficient (R^2) values determined by using the equations of kinetic models were summarized in Table S2. The R^2 revealed that the release behaviour of samples did not fit with neither zero/first order kinetics nor Higuchi model. These results supported that the release of Vitamin-A acetate from nanofibrous webs was not time dependent and did not happen from a non-soluble matrix in water.⁴⁸ On the other hand, samples showed relatively higher consistency with Korsmeyer–Peppas model and it also enables to calculate the diffusion exponent (n) value (Table S2). For Vitamin-A acetate/CD-NW, the n values were determined in the range of 0.45 $<n<$ 0.89 suggesting the irregular or non-Fickian diffusion which could explain the diffusion and erosion-controlled based release of Vitamin-A acetate from nanofibrous webs.⁴⁸ In short, the dissolution and release test findings are also correlated with the XRD and DSC data in which the uncomplexed Vitamin-A acetate parts in Vitamin-A acetate/HP γ CD-NW were detected precisely. As it will be addressed in the following phase solubility part, Vitamin-A acetate form more favourable complexes with HP β CD compared to HP γ CD which might also lead to more efficient inclusion complex formation in the highly concentrated solution of Vitamin-A acetate/HP β CD.

The disintegration of Vitamin-A acetate/CD-NW was further examined on wetted filter paper in order to mimic the oral cavity.⁴⁹ Fig. 9 and Video S2 indicate the disintegration profile of Vitamin-A acetate/CD-NW. Both Vitamin-A acetate/HP β CD-NW and Vitamin-A acetate/HP γ CD-NW tend to disintegrate upon the contact with artificial saliva. Even, Vitamin-A acetate/HP γ CD-NW contain uncomplexed/crystalline Vitamin-A acetate parts, this situation did not reflect on the disintegration results. Such that, the complete disintegration of Vitamin-A acetate/HP β CD-NW outlasted compared to Vitamin-A acetate/HP γ CD-NW and the reason might be the less soluble nature of Vitamin-A acetate/HP β CD inclusion complexes

compared to Vitamin-A acetate/HP γ CD ones which was also observed in the previous dissolution test. Here, the high water solubility of the hydroxypropylated derivatives of HP β CD and HP γ CD is an essential dynamic for the high dissolution and disintegration rate of Vitamin-A acetate/CD-NW.⁵⁸ Besides, high surface area and highly porous feature of nanofibrous webs are other key points which ensure the penetration and interaction of water through the nanofibers.⁵⁹ Therefore, the nanoporous structure of Vitamin-A acetate/CD-NW can create an easy penetration path for saliva in the mouth, the highly soluble nature of modified CD (HP β CD and HP γ CD) and the inclusion complex entity can run the fast release of Vitamin-A acetate by rapid-dissolution of nanofibrous webs.

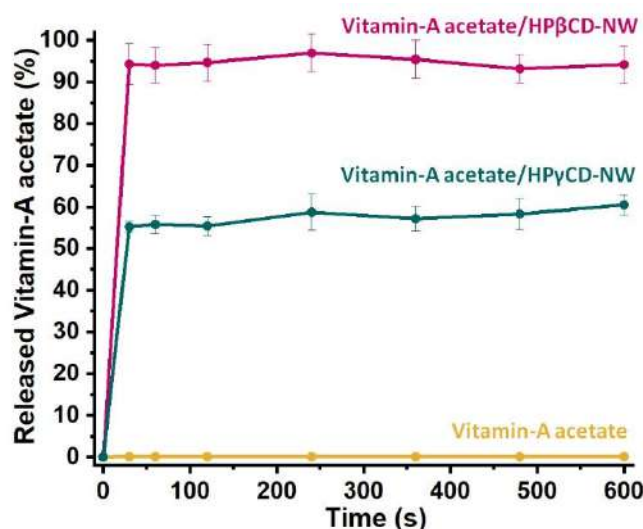


Fig. 8 Time dependent release profiles of Vitamin-A acetate powder, Vitamin-A acetate/HP β CD-NW and Vitamin-A acetate/HP γ CD-NW.

3.4. Phase solubility test

The phase solubility is a precise test in order to get information about the inclusion stoichiometry, binding constant (K_s) and the solubility improvement arises in case of the interaction between CD and guest molecules.^{50,60} Here, Vitamin-A acetate/CD systems were stirred for 24 hours to provide a proper dynamic equilibrium for the inclusion complexation and the filtered aliquot of each these systems were analysed using UV-Vis spectrometer. Fig. 10A indicates the phase solubility diagrams of both Vitamin-A acetate/HP β CD and Vitamin-A acetate/HP γ CD systems plotted for the different CD concentrations. It is obvious from the graphs that the solvated Vitamin-A acetate amount increases linearly against the increasing CD concentrations (0-40 mM). This linear profile represents the AL type phase solubility diagram which reveals the inclusion complex formation with 1:1 (guest:CD) stoichiometry.⁵⁰ On the other, as it was reported previously by Muñoz-Botella et al., Vitamin-A acetate molecules tend to form inclusion complexes with 1:2 molar ratio (Vitamin-A acetate:CD) for HP β CD.⁴¹ Depending on this finding, we have prepared our electrospinning systems using 1:2 molar ratio which was also more feasible for the fiber formation from the highly concentrated CD solutions. In the mentioned study, Muñoz-

Botella et al. have examined the stoichiometry of the systems using the concentrations of 10 mM for HP β CD and 2-8 mM for Vitamin-A acetate.⁴¹ In our case, the phase solubility analyses were carried out using the more diluted Vitamin-A acetate (1 mM) and more concentrated HP β CD (0-40 mM) systems. Therefore, for the experimental conditions that we have used in phase solubility test, Vitamin-A acetate molecules might interact with the HP β CD cavity in a way that 1:1 complexation takes part. Here, the solubility of Vitamin-A acetate ($\sim 7.5 \mu\text{M}$) was increased by ~ 16.1 and ~ 2.3 times with HP β CD and HP γ CD, respectively. Moreover, the binding constant (K_s) was determined as 387.8 M^{-1} for Vitamin-A acetate/HP β CD system and 41.4 M^{-1} for Vitamin-A acetate/HP γ CD system. These results also demonstrated that Vitamin-A acetate form more favourable and stable inclusion complexes with HP β CD compared to HP γ CD. This is most probably originated from the better size match between HP β CD and Vitamin-A acetate which also ensures a better solubility enhancement for Vitamin-A acetate molecules. These findings are also correlated with the previous analyses in which the uncomplexed Vitamin-A acetate parts were detected in case of Vitamin-A acetate/HP γ CD-NW, while Vitamin-A acetate molecules completely presents in the complexed form for Vitamin-A acetate/HP β CD ones. It is noteworthy that there is a significant variation between samples according to statistical analyses ($p < 0.05$). To the best of our knowledge, the phase solubility test confessed by Higuchi and Connors⁵⁰ has not been studied on for Vitamin-A acetate/CD yet. On the other hand, there are several studies in the literature in which the phase solubility profile of the other retinoid derivatives has been evaluated against HP β CD.^{42,43} In these related studies, K_s values were determined as 266.6 M^{-1} and 13563.2 M^{-1} for all-trans-retinoic acid/HP β CD⁴² and 13-cis-retinoic acid/HP β CD⁴³ systems, respectively for the 1:1 molar ratio.

3.5. Antioxidant activity

The uncontrolled reactive oxygen species and free radicals can create oxidative stresses which induce damages to the biochemical compounds including DNA, lipids, and protein which may result in cardiovascular diseases, diabetes, cancer, faster ageing. The antioxidants can scavenge the radical species which are produced continuously in the biological system, and so their destructive effects can be neutralized.^{36,39,61} The antioxidant potential of Vitamin-A originates from its hydrophobic polyene chain which have conjugated double bonds and can reduce and stabilize singlet oxygen, free and peroxy radicals.^{39,62} In this study, the antioxidant potential of Vitamin-A acetate/HP β CD-NW and Vitamin-A acetate/HP γ CD-NW were evaluated using 2,2-diphenyl-1-picrylhydrazyl (DPPH) scavenging assay. For control, the antioxidant test was also performed for the physical mixtures of Vitamin-A acetate/HP β CD and Vitamin-A acetate/HP γ CD and the powder form of Vitamin-A acetate. As it was reported in our previous study, pristine HP β CD and HP γ CD does not have a radical scavenging property.²¹ Fig. 10B indicates the inhibition graphs (%) of all samples for the different time periods of 6, 15 and 24

hours. Moreover, the representative UV-Vis absorption graphs of the antioxidant test recorded for 24 hours were depicted in Fig. 10C along with their representative solution photos.

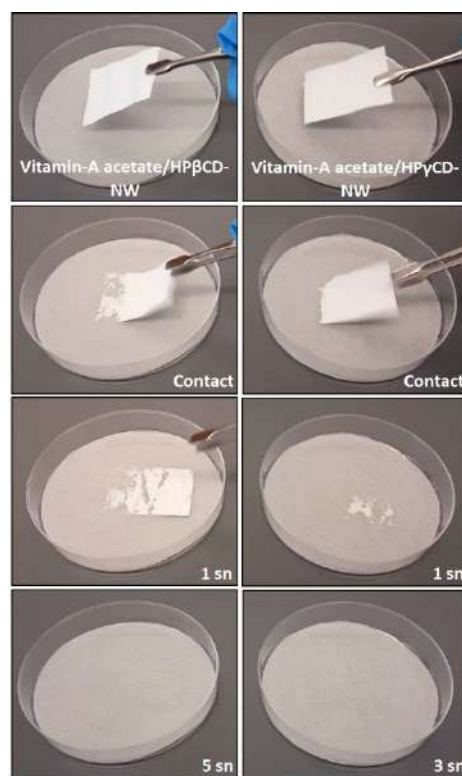


Fig. 9 The disintegration behaviour of samples in saliva simulation. Vitamin-A acetate/HP β CD-NW and Vitamin-A acetate/HP γ CD-NW. These pictures were captured from Video S2.

As it is seen, the antioxidant activity of each samples increases slightly in 15 hours and the scavenging performance of Vitamin-A acetate/HP β CD-NW have stabilized by reaching the inhibition value of $\sim 100\%$. It is also obvious that there is not a distinct difference between 15- and 24-hours results for other samples, as well. These findings are also represented by UV-Vis graphs in which the absorbance intensity of DPPH at 517 nm decreased or disappeared and the colour of the solutions turned into yellow/yellow-purple depending on the scavenging performance of the samples (Fig. 10C). Vitamin-A acetate has quite poor solubility in water, so it could indicate quite low antioxidant activity with the maximum $4.5 \pm 2.0\%$ inhibition in the given period (Fig. 10B). On the other hand, Vitamin-A acetate/HP β CD-NW and Vitamin-A acetate/HP γ CD-NW showed $99.8 \pm 0.3\%$ and $51.6 \pm 8.0\%$ antioxidant activity, respectively due to inclusion complexation. Briefly, Vitamin-A acetate/HP β CD-NW provided the maximum antioxidant activity of $\sim 100\%$ and Vitamin-A acetate/HP γ CD-NW showed lower performance ($51.6 \pm 8.0\%$) for the same sample amount ($\sim 30 \text{ mg}$). As it was discussed in the previous analyses, there is uncomplexed Vitamin-A acetate in Vitamin-A acetate/HP γ CD-NW and this part could not join the radical scavenging, since it was removed by the filtration prior the incubation period. This finding is also correlated with the phase solubility, dissolution and release test results where HP β CD based samples indicated higher solubilizing effect and release % for

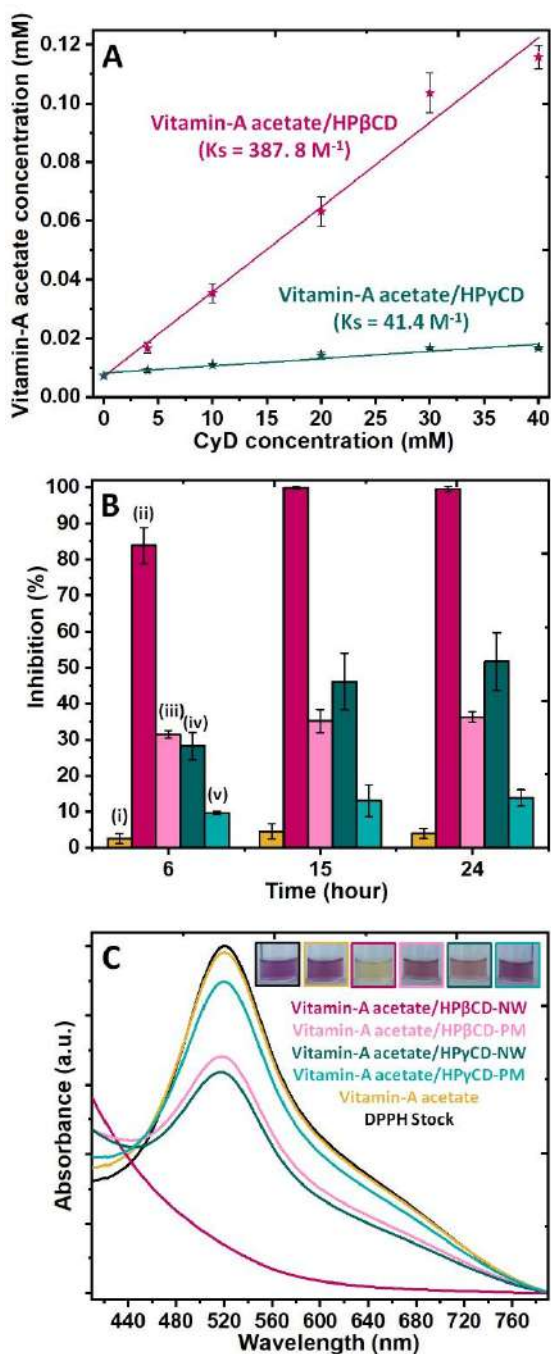


Fig. 10 (A) The phase solubility diagrams of Vitamin-A acetate/HPβCD and Vitamin-A acetate/HPγCD systems. (B) Time dependent antioxidant activity graphs of Vitamin-A acetate powder (i), Vitamin-A acetate/HPβCD-NW (ii), Vitamin-A acetate/HPβCD-PM (iii), Vitamin-A acetate/HPγCD-NW (iv) and Vitamin-A acetate/HPγCD-PM (v). (C) The representative UV-Vis spectra and the photos of the aqueous solutions of DPPH stock and the samples (24 hours).

Vitamin-A acetate compared to HPγCD based samples due to more favourable complex formation between Vitamin-A acetate and HPβCD. As it is observed in Fig. 10B-C, the physical mixtures of Vitamin-A acetate/HPβCD (36.3 ± 1.3 %) and Vitamin-A acetate/HPγCD (13.8 ± 2.3 %) indicated lower antioxidant activity

compared to Vitamin-A acetate/CD-NW because of the uncomplexed state of Vitamin-A acetate present in the physical mixtures. Even so, the antioxidant performance of the physical mixtures might be considered higher than it was supposed to be, because the physical mixtures of Vitamin-A acetate/CD have higher antioxidant performance than the pure Vitamin-A acetate (4.5 ± 2.0 %). However, it should not be forgotten that, the physical mixtures have been prepared with the initial Vitamin-A acetate content of ~ 10 % (w/w), on the other hand Vitamin-A acetate/CD-NW have been obtained by the Vitamin-A acetate content of ~ 5 % (w/w). Thus, even Vitamin-A acetate/CD-NW contain lower amount of Vitamin-A acetate compared to their physical mixtures, they have indicated higher antioxidant property. The reason for the better performance of physical mixtures compared to pristine Vitamin-A acetate powder might be also due to the Vitamin-A acetate/CD inclusion complexes formed during the stirring of physical mixtures which has been performed prior the incubation. The formed Vitamin-A acetate/CD inclusion complexes in the solution of physical mixtures were most probably not removed by the filtration and they have taken place in the scavenging process. As it was expected, the higher complexation efficiency of HPβCD has also showed its effect in case of physical mixtures and Vitamin-A acetate/HPβCD system (36.3 ± 1.3 %) indicated higher performance than Vitamin-A acetate/HPγCD system (13.8 ± 2.3 %). To conclude, the complex formation with CD cavity provided an enhanced solubility and stabilization for Vitamin-A acetate and so higher amount of active compound could join the inhibition of DPPH radical and this suggests the improved antioxidant performance of Vitamin-A acetate. The statistical analyses demonstrated the significant variations between samples ($p < 0.05$).

Conclusions

To conclude, electrospinning is a feasible method in order to encapsulate different kinds of active compounds in the nanofibrous webs. On the other hand, the solubility, stability, and bioavailability of these active compounds can be improved by forming inclusion complexes with cyclodextrin (CD) molecules. The combination of these two phenomena enables to produce the functional nanofibrous webs from the CD inclusion complexes of the variety of compounds which can be utilized as an encapsulation substance and can offer enhanced properties for these active compounds by complexation. Here, the polymer-free inclusion complex nanofibers of Vitamin-A acetate were obtained using two different derivatives of CD (HPβCD and HPγCD). For both CD types, self-standing nanofibrous webs were attained with uniform morphology. The loading capacity of the ultimate Vitamin-A acetate/CD nanofibrous webs (NW) were determined as 5 % (w/w, with respect to total sample amount). The water solubility of the poorly soluble Vitamin-A acetate has been significantly improved in case of both HPβCD and HPγCD nanofiber systems. Additionally, both Vitamin-A acetate/CD nanofibrous webs indicated fast-release profile in liquid medium and fast-disintegration profile in saliva simulation. Moreover, the antioxidant property of Vitamin-A acetate was meaningfully enhanced in case of Vitamin-A acetate/CD-NW. It was found that, HPβCD form more favourable inclusion complexes with

Vitamin-A acetate and so, it provides distinctly higher improvement for both the water solubility and antioxidant property of Vitamin-A acetate compared to HP γ CD. Additionally, the polymer-free Vitamin-A acetate/CD-NW produced in water without using an additional toxic solvent or chemicals are quite promising materials for the food and pharmaceutical based applications. Here, we early reported the generation of polymer-free electrospun nanofibrous webs of Vitamin-A acetate/CD inclusion complexes which have free-standing, flexible, lightweight, and foldable character. In this study, we aimed to integrate the unique properties of both cyclodextrin inclusion complexes and the electrospun nanofiber to develop a new generation food/dietary supplements having orally fast-dissolving properties and nanofibrous web structure.

Conflicts of interest

There are no conflicts of interest to declare.

Acknowledgements

This work made use of the Cornell Center for Materials Research Shared Facilities which are supported through the NSF MRSEC program (DMR-1719875), and the Cornell Chemistry NMR Facility supported in part by the NSF MRI program (CHE-1531632), and the Department of Fiber Science & Apparel Design facilities. Prof. Uyar acknowledges the startup funding from the College of Human Ecology at Cornell University. The partial funding for this research was also graciously provided by Nixon Family (Lea and John Nixon) thru College of Human Ecology at Cornell University.

References

- M. I. Dias, I. C. F. R. Ferreira and M. F. Barreiro, *Food Funct.*, 2015, **6**, 1035–1052.
- G. Wadhwa, S. Kumar, L. Chhabra, S. Mahant and R. Rao, *J. Incl. Phenom. Macrocycl. Chem.*, 2017, **89**, 39–58.
- P. N. Ezhilarasi, P. Karthik, N. Chhanwal and C. Anandharamkrishnan, *Food Bioprocess Technol.*, 2013, **6**, 628–647.
- J. A. Bhushani and C. Anandharamkrishnan, *Trends Food Sci. Technol.*, 2014, **38**, 21–33.
- P. Wen, Y. Wen, M.-H. Zong, R. J. Linhardt and H. Wu, *J. Agric. Food Chem.*, 2017, **65**, 9161–9179.
- M. R. Rostami, M. Yousefi, A. Khezerlou, M. A. Mohammadi and S. M. Jafari, *Food Hydrocoll.*
- P. Wen, M.-H. Zong, R. J. Linhardt, K. Feng and H. Wu, *Trends food Sci. Technol.*, 2017, **70**, 56–68.
- R. Leidy and Q.-C. M. Ximena, *Trends food Sci. Technol.*
- T. S. M. Kumar, K. S. Kumar, N. Rajini, S. Siengchin, N. Ayrlimis and A. V. Rajulu, *Compos. Part B Eng.*, 2019, 107074.
- T. D. Brown, P. D. Dalton and D. W. Hutmacher, *Prog. Polym. Sci.*, 2016, **56**, 116–166.
- J. Xue, T. Wu, Y. Dai and Y. Xia, *Chem. Rev.*, 2019, **119**, 5298–5415.
- A. Celebioglu, Z. I. Yildiz and T. Uyar, *J. Agric. Food Chem.*, 2018, **66**, 457–466.
- A. Celebioglu, Z. I. Yildiz and T. Uyar, *Food Res. Int.*, 2018, **106**, 280–290.
- A. Celebioglu, Z. Aytac, M. E. Kilic, E. Durgun and T. Uyar, *J. Mater. Sci.*, 2018, **53**, 5436–5449.
- A. Celebioglu, Z. I. Yildiz and T. Uyar, *Int. J. food Sci. Technol.*, 2018, **53**, 112–120.
- Z. Aytac, A. Celebioglu, Z. Yildiz and T. Uyar, *Nanomaterials*, 2018, **8**, 793.
- Z. I. Yildiz, A. Celebioglu, M. E. Kilic, E. Durgun and T. Uyar, *J. Mater. Sci.*, 2018, **53**, 15837–15849.
- Z. I. Yildiz, A. Celebioglu, M. E. Kilic, E. Durgun and T. Uyar, *J. Food Eng.*, 2018, **224**, 27–36.
- A. Celebioglu, F. Kayaci-Senirmak, S. İpek, E. Durgun and T. Uyar, *Food Funct.*, 2016, **7**, 3141–3153.
- A. Celebioglu and T. Uyar, *J. Agric. Food Chem.*, 2017, **65**, 5404–5412.
- A. Celebioglu and T. Uyar, *Food Chem.*, 2020, **317**, 126397.
- A. Celebioglu and T. Uyar, *J. Agric. Food Chem.*
- A. Celebioglu and T. Uyar, *Int. J. Pharm.*, 2020, 119395.
- A. Celebioglu and T. Uyar, *RSC Med. Chem.*
- A. Celebioglu and T. Uyar, *Int. J. Pharm.*, 2019, 118828.
- A. Celebioglu and T. Uyar, *Mol. Pharm.*
- Z. I. Yildiz, A. Celebioglu and T. Uyar, *Int. J. Pharm.*, 2017, **531**, 550–558.
- G. Astray, C. Gonzalez-Barreiro, J. C. Mejuto, R. Rial-Otero and J. Simal-Gandara, *Food Hydrocoll.*, 2009, **23**, 1631–1640.
- P. Jansook, N. Ogawa and T. Loftsson, *Int. J. Pharm.*, 2018, **535**, 272–284.
- H. M. C. Marques, *Flavour Fragr. J.*, 2010, **25**, 313–326.
- E. Fenyvesi, M. Vikmon and L. Szente, *Crit. Rev. Food Sci. Nutr.*, 2016, **56**, 1981–2004.
- G. F. Combs Jr and J. P. McClung, *The vitamins: fundamental aspects in nutrition and health*, Academic press, 2016.
- Y. O. Li, V. P. D. González and L. L. Diosady, in *Microencapsulation in the Food Industry*, Elsevier, 2014, pp. 501–522.
- A. J. Meléndez-Martínez, *Mol. Nutr. Food Res.*, 2019, **63**, 1801045.
- I. T. Khan, M. Nadeem, M. Imran, R. Ullah, M. Ajmal and M. H. Jaspal, *Lipids Health Dis.*, 2019, **18**, 41.
- X. Wu, J. Cheng and X. Wang, *Nutr. Cancer*, 2017, **69**, 521–533.
- S. Iqbal and I. Naseem, *Nutrition*, 2015, **31**, 901–907.
- W. Chen, S. Zhao, W. Zhu, L. Wu and X. Chen, *Arch. Immunol. Ther. Exp. (Warsz.)*, 2019, 1–11.
- V. P. Palace, N. Khaper, Q. Qin and P. K. Singal, *Free Radic. Biol. Med.*, 1999, **26**, 746–761.
- E. Pinho, M. Grootveld, G. Soares and M. Henriques, *Carbohydr. Polym.*, 2014, **101**, 121–135.
- S. Munoz-Botella, M. A. Martin, B. Del Castillo, D. A. Lerner and J. C. Menendez, *Anal. Chim. Acta*, 2002, **468**, 161–170.
- H. Lin, S. Y. Chan, K. S. Y. Low, M. L. Shoon and P. C. Ho, *J.*

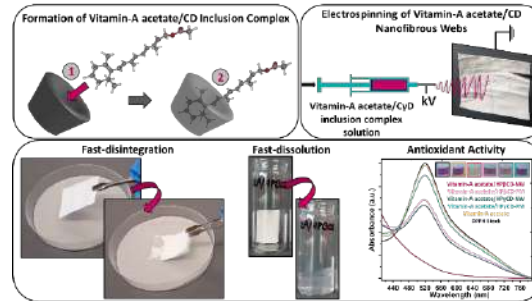
ARTICLE

Journal Name

- Pharm. Sci.*, 2000, **89**, 260–267.
- 43 K. L. Yap, X. Liu, J. C. Thenmozhiyal and P. C. Ho, *Eur. J. Pharm. Sci.*, 2005, **25**, 49–56.
- 44 P. Taepaiboon, U. Rungsardthong and P. Supaphol, *Eur. J. Pharm. Biopharm.*, 2007, **67**, 387–397.
- 45 H. Li, M. Wang, G. R. Williams, J. Wu, X. Sun, Y. Lv and L.-M. Zhu, *RSC Adv.*, 2016, **6**, 50267–50277.
- 46 A. Fahami and M. Fathi, *Food Hydrocoll.*, 2018, **81**, 31–38.
- 47 S. M. Lemma, M. Scampicchio, P. J. Mahon, I. Sbarski, J. Wang and P. Kingshott, *J. Agric. Food Chem.*, 2015, **63**, 3481–3488.
- 48 N. A. Peppas and B. Narasimhan, *J. Control. Release*, 2014, **190**, 75–81.
- 49 Y. Bi, H. Sunada, Y. Yonezawa, K. Danjo, A. Otsuka and K. IIDA, *Chem. Pharm. Bull.*, 1996, **44**, 2121–2127.
- 50 T. Higuchi and K. A. Connors, *Adv Anal Chem Instrum*, 1965, **4**, 117–212.
- 51 T. Uyar and F. Besenbacher, *Polymer (Guildf.)*, 2008, **49**, 5336–5343.
- 52 G. Narayanan, R. Boy, B. S. Gupta and A. E. Tonelli, *Polym. Test.*, 2017, **62**, 402–439.
- 53 P. Mura, *J. Pharm. Biomed. Anal.*, 2015, **113**, 226–238.
- 54 C. Yuan, B. Liu and H. Liu, *Carbohydr. Polym.*, 2015, **118**, 36–40.
- 55 E. I. Taha, S. Al-Saidan, A. M. Samy and M. A. Khan, *Int. J. Pharm.*, 2004, **285**, 109–119.
- 56 N. L. Rockley, M. G. Rockley, B. A. Halley and E. C. Nelson, in *Methods in enzymology*, Elsevier, 1986, vol. 123, pp. 92–101.
- 57 A. Celebioglu and T. Uyar, *Nanoscale*, 2012, **4**, 621–631.
- 58 T. Loftsson and M. E. Brewster, *J. Pharm. Pharmacol.*, 2010, **62**, 1607–1621.
- 59 D.-G. Yu, J.-J. Li, G. R. Williams and M. Zhao, *J. Control. release*.
- 60 M. E. Brewster and T. Loftsson, *Adv. Drug Deliv. Rev.*, 2007, **59**, 645–666.
- 61 I. Gülçin, *Arch. Toxicol.*, 2012.
- 62 C. Grażyna, C. Hanna, A. Adam and B. M. Magdalena, *Int. J. Dairy Technol.*, 2017, **70**, 165–178.

View Article Online
DOI: 10.1039/D0FO01776K

Table of content



The polymer-free inclusion complex nanofibers of Vitamin-A acetate/Cyclodextrin having fast-dissolving and enhanced antioxidant property for the purpose of new generation food/dietary supplement system.